

REGULAR PAPER

Functionalized GaN/GaN heterostructures for hydrogen sulfide sensing

To cite this article: Jassim Shahbaz *et al* 2019 *Jpn. J. Appl. Phys.* **58** SC1028

View the [article online](#) for updates and enhancements.

You may also like

- [Recombination dynamics in GaN/GaN quantum wells](#)
Andreas Hangleiter
- [Growth of 300-nm-thick epitaxial AlInN films on a semi-relaxed c-plane GaInN template by metalorganic chemical vapor deposition](#)
Makoto Miyoshi, Mizuki Yamanaka, Takashi Egawa *et al.*
- [GaN-based tunnel junctions and optoelectronic devices grown by metal-organic vapor-phase epitaxy](#)
Tetsuya Takeuchi, Satoshi Kamiyama, Motoaki Iwaya *et al.*



Functionalized GaN/GaN heterostructures for hydrogen sulfide sensing

Jassim Shahbaz^{1*}, Martin Schneidereit¹, Klaus Thonke², and Ferdinand Scholz¹

¹Institute of Functional Nanosystems, Ulm University, D-89069 Ulm, Germany

²Institute of Quantum Matter/Semiconductor Physics Group, Ulm University, D-89069 Ulm, Germany

*E-mail: jassim.shahbaz@uni-ulm.de

Received December 31, 2018; accepted March 12, 2019; published online May 17, 2019

Near-surface GaN/GaN quantum wells (QWs) were investigated as optical transducers for the detection of hydrogen sulfide. The heterostructure sensors were grown by metal organic vapor phase epitaxy and later covered by a thin layer of Au by electron beam evaporation. The QW photoluminescence (PL) is sensitive to changes in the sensor surface potential. By the adsorption of hydrogen sulfide (H₂S) on the Au cover layer, downward near-surface band bending results in an increase of the quantum confined Stark effect in the GaInN QW producing a red shift in its luminescence. Unexpectedly, an increase in PL intensity is also observed. A concentration of 0.01 parts per million of H₂S in nitrogen has been successfully detected. This phenomenon may be helpful to detect trace amounts of H₂S present in the human breath for early detection of diseases. © 2019 The Japan Society of Applied Physics

1. Introduction

Group-III nitrides have well known material properties that make them suitable for application in chemical and biochemical sensing.^{1–5} Specifically, GaN has the capacity to operate at high temperatures, hence it can be used to realize Schottky diode and field effect transistor gas sensors.^{6–11} Due to its surface being highly electrochemically stable,^{11–14} GaN also may find applications in the field of biochemical sensors in liquid electrolytes.^{15–18} The material also has good optoelectronic properties that can be utilized in the creation of novel sensors which produce an optical readout signal. Since this optical signal can be processed remotely, the sensor can be used in situations where destructive chemicals would make electrical contacting a complicated endeavor. Optical readout also provides the opportunity to use a single sensor with different functionalization to detect different molecules at the same time.

GaN based gas sensors investigated in this study work on the principle of changes in the near-surface band bending related to the change of surface charges induced by the adsorption or desorption of gas molecules on the sensor surface. This in turn results in a change of photoluminescence (PL) emission, easily detectable even at room temperature. A typical near-surface upward band bending of about 1 eV has been reported for n-doped GaN.^{19,20} This partially compensates the quantum confined Stark effect (QCSE) caused by the piezoelectric and spontaneous polarizations in a GaInN quantum well (QW) placed just a few nanometers below the surface. When a reducing agent like hydrogen attaches to the semiconductor surface, it will transfer an electron to the semiconductor resulting in the formation of an electric field and subsequently downward band bending will occur.²¹ This finally results in an increase of the QCSE and a red shift in the QW PL emission, whereas in contrary an oxidizing agent which removes an electron from the surface will induce a blue shift.²² However, this exchange of electrons is not very straightforward in the presence of a metal layer on the semiconductor surface.

This study is concerned with characterizing GaN/GaN QW heterostructures grown on an optically transparent sapphire substrate and capped by a thin metal layer to achieve improved selectivity. As discussed above, chemically induced changes to the surface potential alter the PL emission

wavelength and intensity of the heterostructure. This effect is used here to demonstrate gas sensing. Hydrogen sulfide (H₂S) is of particular interest in the medical sciences community, as accurate detection of the gas in the exhaled human breath can provide useful information about a patient's health.^{23–28} Our studies have shown that a layer of gold on top of the GaN/GaN heterostructure provides very good sensitivity for H₂S. Concentrations as low as 0.01 parts per million (ppm) of H₂S in nitrogen have been detected with the sensor. In accordance with simulation results, a thinner GaN cap layer on top of the GaInN QW proved to be more sensitive. The sensitivity was further increased by introducing n-type doping during GaN growth.

2. Experimental methods

For the growth of GaN/GaN semiconductor heterostructure investigated in this work, an Aixtron AIX200/RF HT commercial horizontal flow metal organic vapor phase epitaxy reactor was used. Ammonia (NH₃), trimethylgallium (TMGa), trimethylaluminum (TMAI), triethylgallium (TEGa), and trimethylindium (TMIn) are the precursors for the epitaxial growth. Silane gas is used as Si source for n-type doping. Ultra-pure nitrogen and hydrogen are used as carrier gases. Epitaxial growth takes place on a 2 inch *c*-oriented double-side polished sapphire wafer with 0.2° offcut towards the *m*-direction. A 20 nm thick AlN nucleation layer is firstly grown for better GaN crystal quality.²⁹ This is followed by Ga-polar GaN buffer layer growth with a thickness of 1.2 μm at 1135 °C. This buffer layer was either left undoped, or different levels of n-type doping ($\approx 1 \times 10^{17} \text{ cm}^{-3}$ – $1 \times 10^{19} \text{ cm}^{-3}$) were added by the inclusion of silane during the growth process. A single 3 nm thick GaInN QW containing about 13% of indium and emitting at about 440 nm is grown at a temperature of 845 °C on top of the buffer with an undoped GaN capping layer of varying thickness, i.e. 3, 6 and 9 nm (Fig. 1). For better detection of hydrogen and hydrogen sulfide, the sensor surface is functionalized with a few nm thick metal layer of either Pt or Au using electron beam evaporation.

To perform optical sensing experiments, the sample was placed in a gas sensing setup (Fig. 2), which consists of a sealed chamber and a sample holder used for backside excitation of the sample through a glass window with anti-reflective coating. The chamber is connected to a gas mixing

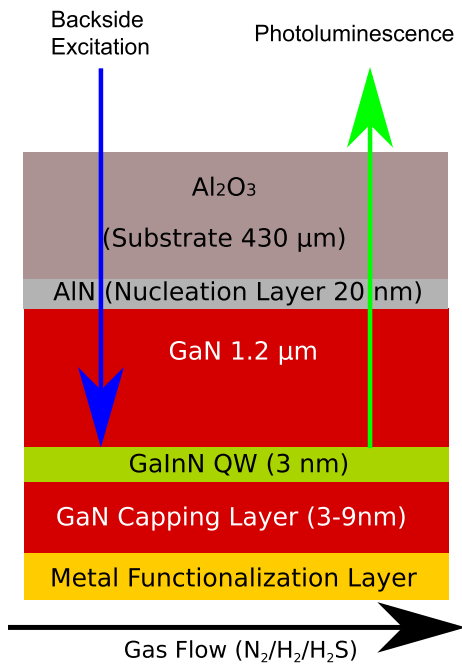


Fig. 1. (Color online) Cross section of the GaN/GaNIn semiconductor heterostructure. Varying background doping and capping layers of different thickness were used for the measurements.

apparatus with a supply of nitrogen, forming gas (5% hydrogen in 95% nitrogen) and H₂S (10 ppm in nitrogen). The sensor is first exposed to 500 sccm of nitrogen for 5 min for initialization. Then H₂S diluted by nitrogen is introduced in the chamber for 5 min to measure the change in PL response from the sensor. Several cycles of this switching between nitrogen and hydrogen sulfide (diluted in nitrogen) are repeated. A blue laser with a wavelength of 405 nm is used for selective QW excitation. The readout of the sensor response is performed through the same path as the laser used for excitation. A dichroic mirror with a cut-off wavelength of 425 nm separates the PL from the excitation. A monochromator in combination with a CCD camera is used to spectrally resolve the PL emission, which is continuously recorded during the gas switching. The QW peak wavelength and intensity are evaluated as the sensor signal.

3. Results and discussion

A set of samples with undoped GaN buffer and a single GaInN QW were first used for hydrogen sulfide sensing. We investigated the influence of the GaN cap layer thickness which has a direct relation to the sensitivity of the sensor. The GaInN QW should be located close to the surface within the depletion zone to maximize the wavelength shift. However,

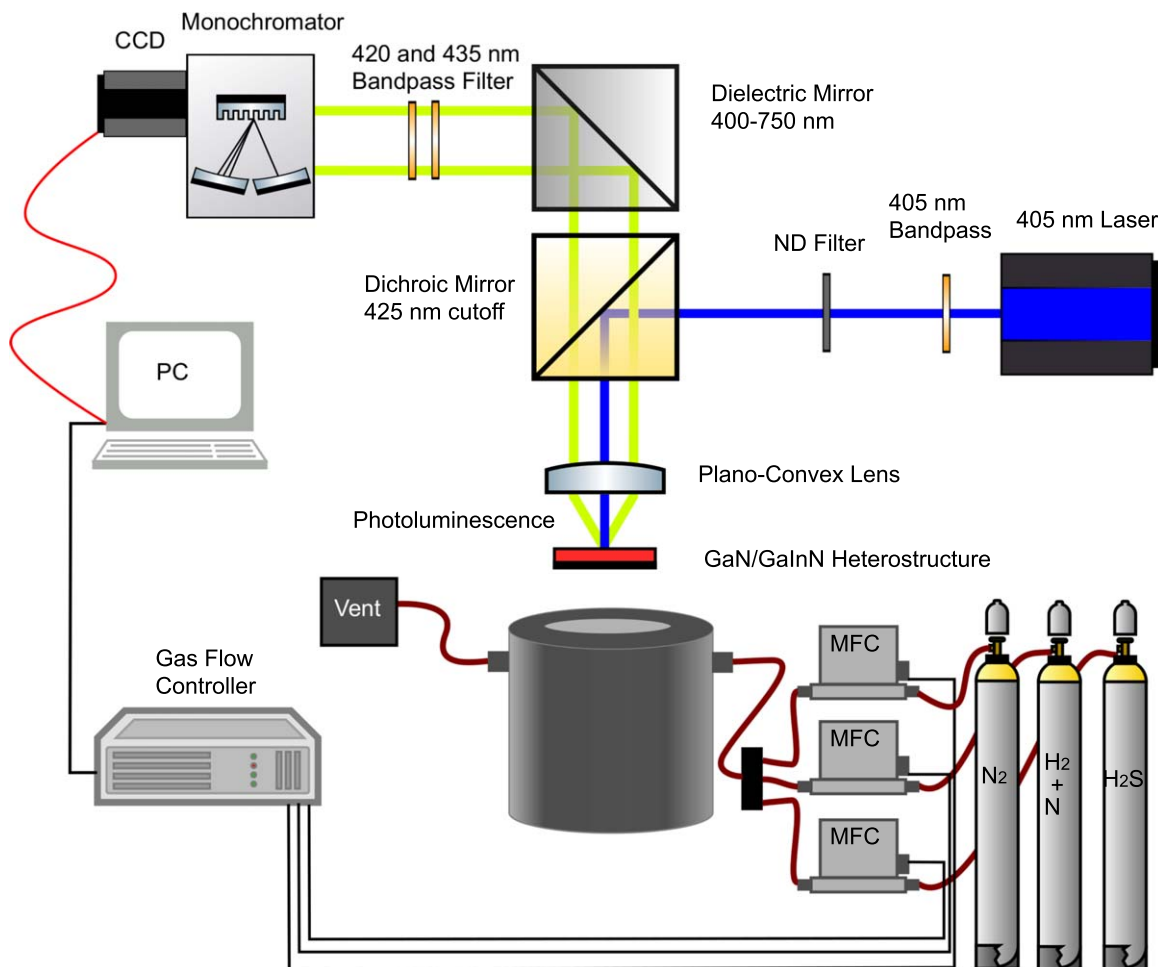


Fig. 2. (Color online) Optical gas sensing setup: a blue laser (405 nm) is used for the QW excitation. The sealed chamber is connected to a gas mixing setup with a supply of nitrogen, hydrogen and hydrogen sulfide.

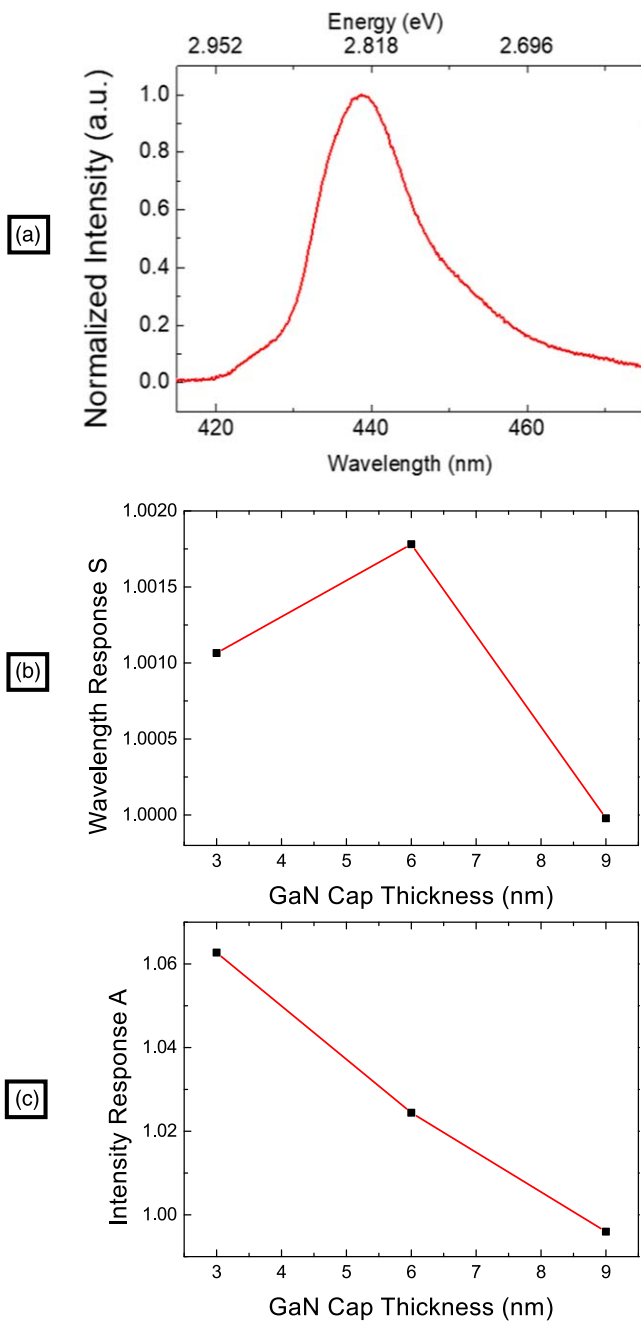


Fig. 3. (Color online) (a) Reference PL spectrum of a sensor (b) wavelength and (c) intensity response of Au functionalized sensor with cyclic switching of nitrogen and 10 ppm H₂S.

the closer the QW is to the surface, the more likely electrons will tunnel out and non-radiatively recombine via surface states. Therefore, a compromise needs to be achieved between the sensitivity and the signal-to-noise ratio.

The influence of GaN cap layers of different thickness was investigated by letting nitrogen and 10 ppm of H₂S cyclically switch in 5 min intervals. A gold layer of 3 nm thickness on top of the GaN cap layer is used for functionalization of the sensor for H₂S detection due to the strong chemical affinity between Au and S.³⁰⁾ At room temperature, the adsorbed H₂S molecules on the Au layer may decompose and form SH species, while H₂ molecules are released to the gas phase.³¹⁾ This chemisorption at the sensor surface leads to a change in the PL wavelength and intensity. Another probable reason for the PL shift could be the diffusion of atomic hydrogen

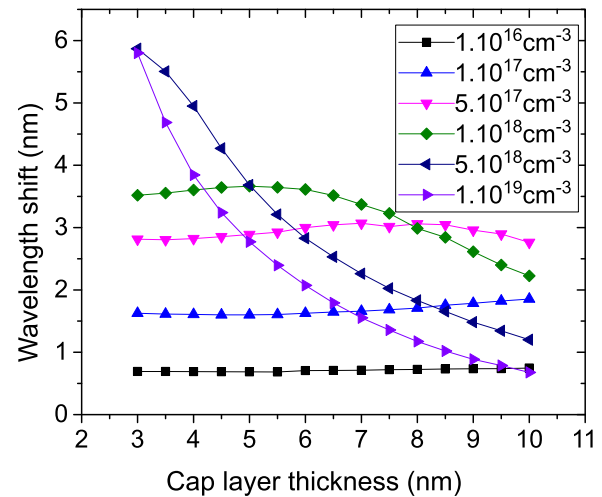


Fig. 4. (Color online) Simulated data (nextnano) showing a higher sensitivity with more doping and thinner GaN cap layer.

through the GaN/Au interface to passivate the surface defects or form interface dipoles leading to a change in the Schottky barrier height. However, further investigations of these phenomena are currently done for a better understanding.

A reference PL spectrum is shown in Fig. 3(a) with a peak wavelength of 439 nm. The dependence of the wavelength response ($S = \lambda_G/\lambda_N$) and the intensity response ($A = I_G/I_N$) on the thickness of the cap layer are also plotted in Fig. 3, where λ_G and λ_N are the peak wavelengths in H₂S and N₂ ambient, respectively. Similarly, I_G and I_N are the maximum intensities of the PL emission in the two different gas environments. We find, that an increase in the cap thickness results in a decrease in the wavelength and intensity response. This result confirms the simulation predictions shown in Fig. 4, where the samples with the thinner cap layer are expected to show a larger wavelength shift. The simulations were performed using the software “nextnano”,³²⁾ which yields a self-consistent solution of Poisson, Schrödinger and drift-diffusion current equations. Here, the sensing situation was simulated by evaluating the wavelength response difference of the sensor structure when varying the Fermi level surface pinning by 0.3 eV. The simulation also predicts that by increasing the doping concentration in the sensor the sensitivity can be increased, because higher doping leads to a stronger curvature of the band bending near the surface.

Therefore, a series of samples with different doping concentration was grown, and similar gas sensing experiments were performed. For this series however, a much lower concentration of H₂S was used to determine the lower limit of detection. Figure 5 shows the change in wavelength and intensity over the different gas switching cycles. A small red shift is observed when 1 ppm of H₂S is added to the sensing chamber, and the effect is clearer for the highest doped sample, i.e. $9 \times 10^{18} \text{ cm}^{-3}$. The change in the PL intensity is apparently much more pronounced as the intensity increases by roughly 50% under H₂S ambient for the highest doped sample. The sensor response time is about a minute at room temperature to reach 90% of the maximum intensity, however the sensor recovery takes about 5 min to achieve the starting PL intensity in N₂ ambient. An interesting phenomenon to note here is the increase in PL intensity accompanied with a red shift in the emission wavelength. The band bending caused by the changes

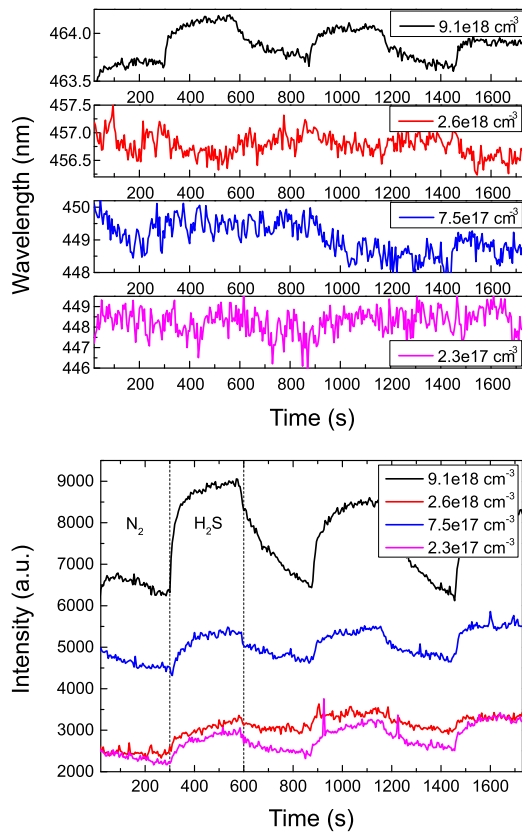


Fig. 5. (Color online) Change in PL wavelength and intensity of a single QW, varying doping concentration samples and with 3 nm Au functionalization. The highest doped samples shows the best sensitivity when switching from nitrogen to hydrogen sulfide ambient.

in the surface potential could possibly increase the QW barrier height toward the GaN bulk effectively stopping the leakage of electrons hence increasing the radiative recombination rate. Another probable explanation, as mentioned previously, is again the diffusion of hydrogen gas to passivate the surface defects leading to an increase in the PL intensity.

To further test the selectivity of the Au functionalization layer towards H₂S, another highly doped sample with the same internal specifications was functionalized with a Pt layer which has previously shown good hydrogen sensing results.³³ Obviously, only the Au functionalization detects hydrogen sulfide even at a lower concentration of 1 ppm (Fig. 6). Pt functionalization fails to detect H₂S and also leads to a considerable decrease in PL intensity presumably due to the tunneling out of electrons as the barrier height is reduced. The decrease in the PL intensity necessitates an increase in excitation power to make the PL signal detectable.

The lowest concentration of H₂S which could be detected with our sensor was 0.01 ppm (10 ppb) as shown in Fig. 7. The intensity and wavelength response are both plotted with a logarithmic *x*-axis showing the decrease in the H₂S concentration from 10 to 0.01 ppm. The intensity response is a better indicator compared to the wavelength response, which changes only slightly. At such low concentrations the sensor response time increased from 60 to about 120 s.

4. Conclusions

The effect of hydrogen sulfide adsorption on the surface of a GaN/GaNN heterostructure with metal functionalization layer has been investigated. A thinner GaN cap layer results

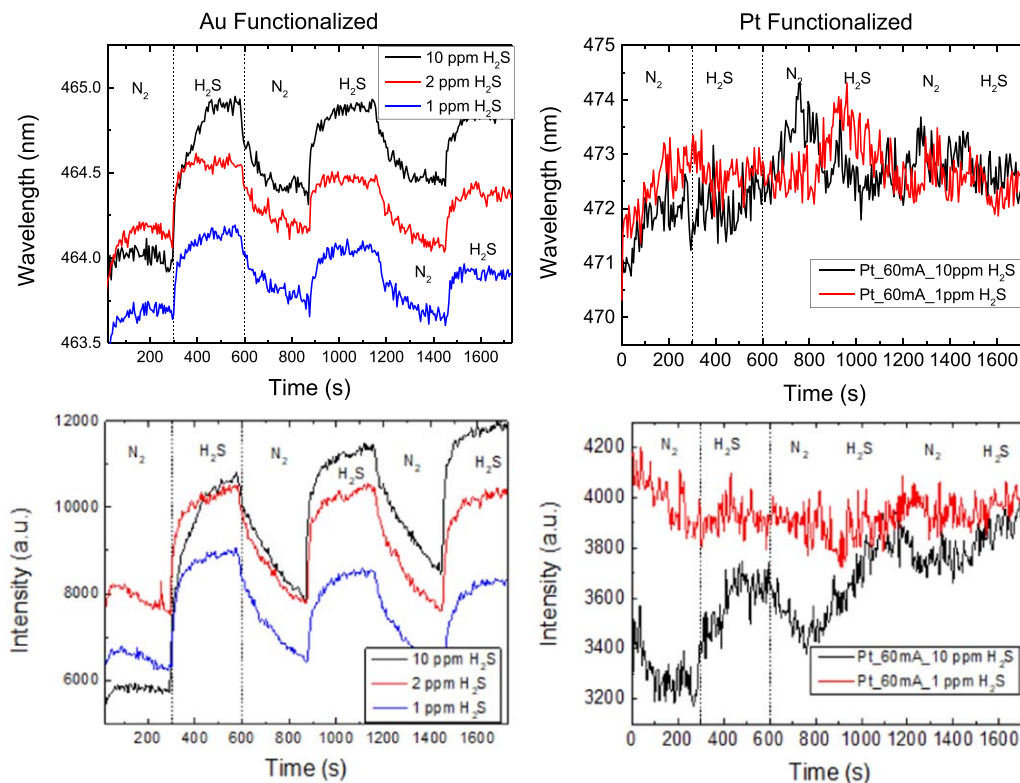


Fig. 6. (Color online) Comparison of Au (left) and Pt (right) functionalization for hydrogen sulfide sensing, Au is able to detect 1 ppm, Pt does not show sensitivity to H₂S even at 10 ppm. A higher excitation power is also necessary to detect the PL as Pt leads to lowering of the signal intensity.

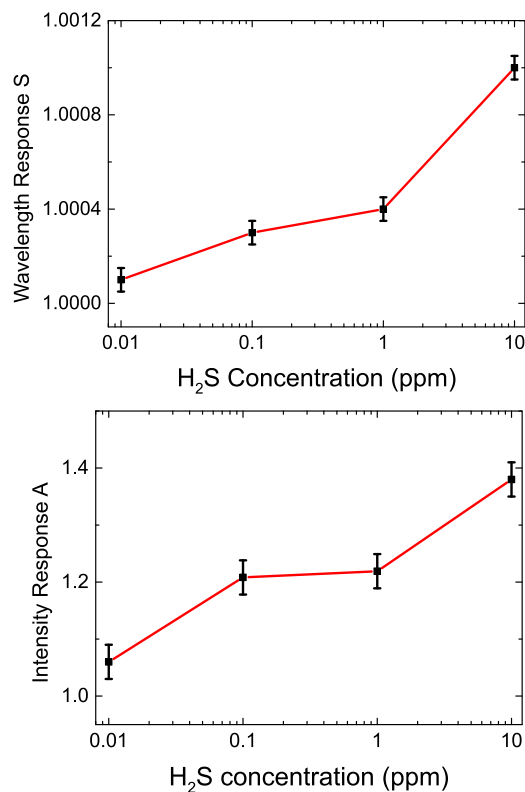


Fig. 7. (Color online) Intensity and wavelength response of a GaN/GaN heterostructure sensor with different concentrations of hydrogen sulfide.

in better sensitivity. Experimental data are consistent with theoretical predictions that higher doping concentration in the bulk layer leads to much better sensitivity. A gold layer was found to be better for H₂S sensing compared to a Pt layer. With the adsorption of H₂S on the Au layer, a red shift and an increase in the emission intensity is observed. This indicates better carrier confinement leading to stronger radiative recombination. The lowest concentration of H₂S detected was 0.01 ppm at room temperature, which is in the range required for breath analysis. The results support the prospective use of GaN/GaN heterostructures in gas sensing applications.

Acknowledgments

The scientific support provided by Florian Huber (Institute of Quantum Matter/Semiconductor Physics Group, Ulm University, Germany) and Peter Radermacher (Institute of Anesthesiological Pathophysiology and Process Development, Ulm University, Germany) is gratefully acknowledged.

This work is financially supported by the Deutsche Forschungsgemeinschaft (DFG) within the graduate school PULMOSENS in the project “Semiconductor-based nano structures for the highly sensitive optical analysis of gases and bio-materials”.

ORCID iDs

Jassim Shahbaz  <https://orcid.org/0000-0003-4763-6121>

- O. Weidemann, P. K. Kandaswamy, E. Monroy, G. Jegert, M. Stutzmann, and M. Eickhoff, *Appl. Phys. Lett.* **94**, 113108 (2009).
- D. Heinz et al., *IEEE J. Sel. Top. Quantum Electron.* **23**, 1900109 (2017).
- J. Teubert, P. Becker, F. Furtmayr, and M. Eickhoff, *Nanotechnology* **22**, 275505 (2011).
- S. J. Pearton, F. Ren, Y. L. Wang, B. H. Chu, K. H. Chen, C. Y. Chang, W. Lim, J. Lin, and D. P. Norton, *Prog. Mater. Sci.* **55**, 1 (2010).
- N. Chaniotakis and N. Sofikiti, *Anal. Chim. Acta* **615**, 1 (2008).
- J. Schalwig, G. Müller, U. Karrer, M. Eickhoff, O. Ambacher, M. Stutzmann, L. Görgens, and G. Dollinger, *Appl. Phys. Lett.* **80**, 1222 (2002).
- K. H. Baik, H. Kim, S. N. Lee, E. Lim, S. J. Pearton, F. Ren, and S. Jang, *Appl. Phys. Lett.* **104**, 072103 (2014).
- O. Weidemann, M. Hermann, G. Steinhoff, H. Wingbrant, A. L. Spetz, M. Stutzmann, and M. Eickhoff, *Appl. Phys. Lett.* **83**, 773 (2003).
- J. Schalwig, G. Müller, M. Eickhoff, O. Ambacher, and M. Stutzmann, *Sens. Actuators B* **87**, 425 (2002).
- F. K. Yam, Z. Hassan, and A. Y. Hudeish, *Thin Solid Films* **515**, 7337 (2007).
- J. Schalwig, G. Müller, M. Eickhoff, O. Ambacher, and M. Stutzmann, *Mater. Sci. Eng. B* **93**, 207 (2002).
- K. Maier, A. Helwig, G. Müller, P. Becker, P. Hille, J. Schörmann, J. Teubert, and M. Eickhoff, *Sens. Actuators B* **197**, 87 (2014).
- Y. L. Wang, F. Ren, U. Zhang, Q. Sun, C. D. Yerino, T. S. Ko, Y. S. Cho, I. H. Lee, J. Han, and S. J. Pearton, *Appl. Phys. Lett.* **94**, 212108 (2009).
- I. Cimalla et al., *Sens. Actuators B* **123**, 740 (2007).
- M. Stutzmann, J. A. Garrido, M. Eickhoff, and M. S. Brandt, *Phys. Status Solidi A* **203**, 3424 (2006).
- S. Paul, A. Helwig, G. Müller, F. Furtmayr, J. Teubert, and M. Eickhoff, *Sens. Actuators B* **173**, 120 (2012).
- G. Steinhoff, M. Hermann, W. J. Schaff, L. F. Eastman, M. Stutzmann, and M. Eickhoff, *Appl. Phys. Lett.* **83**, 177 (2003).
- H. T. Wang, B. S. Kang, F. Ren, S. J. Pearton, J. W. Johnson, P. Rajagopal, J. C. Roberts, E. L. Piner, and K. J. Linthicum, *Appl. Phys. Lett.* **91**, 222101 (2003).
- V. M. Bermudez, *J. Appl. Phys.* **80**, 1190 (1996).
- M. Foussekis, J. D. McNamara, A. A. Baski, and M. A. Reshchikov, *Appl. Phys. Lett.* **101**, 082104 (2012).
- M. Foussekis, A. A. Baski, and M. A. Reshchikov, *Appl. Phys. Lett.* **94**, 162116 (2009).
- Z. Zhang and J. T. Yates Jr., *Chem. Rev.* **112**, 5520 (2012).
- T. Merz et al., *Intensive Care Med. Exp.* **6**, 41 (2018).
- B. Geng, J. Yang, Y. Qi, J. Zhao, Y. Pang, J. Du, and C. Tang, *Biochem. Biophys. Res. Commun.* **313**, 362 (2004).
- J. W. Elrod et al., *Proc. Natl. Acad. Sci. U.S.A.* **104**, 15560 (2007).
- J. W. Calvert, S. Jha, S. Gundewar, J. W. Elrod, A. Ramachandran, C. B. Pattillo, C. G. Kevil, and D. H. Lefer, *Circ. Res.* **105**, 365 (2009).
- K. Kondo et al., *Circulation* **127**, 1116 (2013).
- R. Coletti, G. Almeida-Pereira, L. L. Elias, and J. Antunes-Rodrigues, *Horm. Behav.* **67**, 12 (2015).
- J. Hertkorn, P. Brückner, S. B. Thapa, T. Wunderer, F. Scholz, M. Feneberg, K. Thonke, R. Sauer, M. Beer, and J. Zweck, *J. Cryst. Growth* **308**, 30 (2007).
- D. R. Lide, *CRC Handbook of Chemistry and Physics* (CRC Press, Boca Raton, FL, 1997) 78th ed., p. 9.
- A. J. Leavitt and T. P. Beebe Jr., *Surf. Sci.* **314**, 23 (1994).
- S. Birner, (2018), Nextnano [<https://nextnano.de>].
- J. Shahbaz, M. Schneidereit, B. Hörbrand, S. Bauer, K. Thonke, and F. Scholz, Proc. Europ. Workshop on Metalorganic Vapor Phase Epitaxy, EW-MOVPE17, 2017, p. 118.